

Supplementary Figures

Figure S1 SDS-PAGE analysis of the overexpressed intracellular laccase protein in A_{pGlac} . A_{pGT} was used as the control. Red arrow indicates the laccase protein band, while green arrow denotes the green fluorescent protein located in the laccase operon. Biological triplicates were performed.

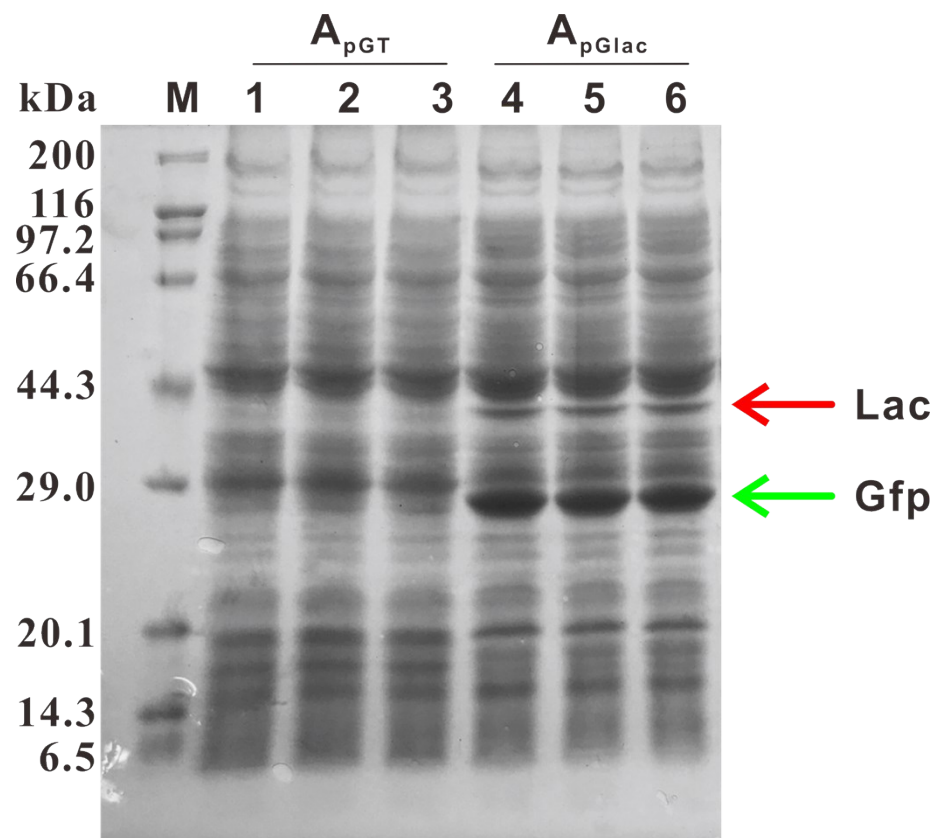


Figure S2 The laccase activity and cell growth of the recombinant A514 strains in TISS strategy. (A) The intracellular laccase activity of A_{pULac} , $A_{pUI-2539}$, and $A_{pUI-2549}$. (B) The growth curves of $A_{pUI-2549}$ under different xylose addition time points. (C) The time point-dependent induction of real-time extracellular laccase activity in $A_{pUI-2549}$. 2 mM xylose (final concentration) was added at different time points.

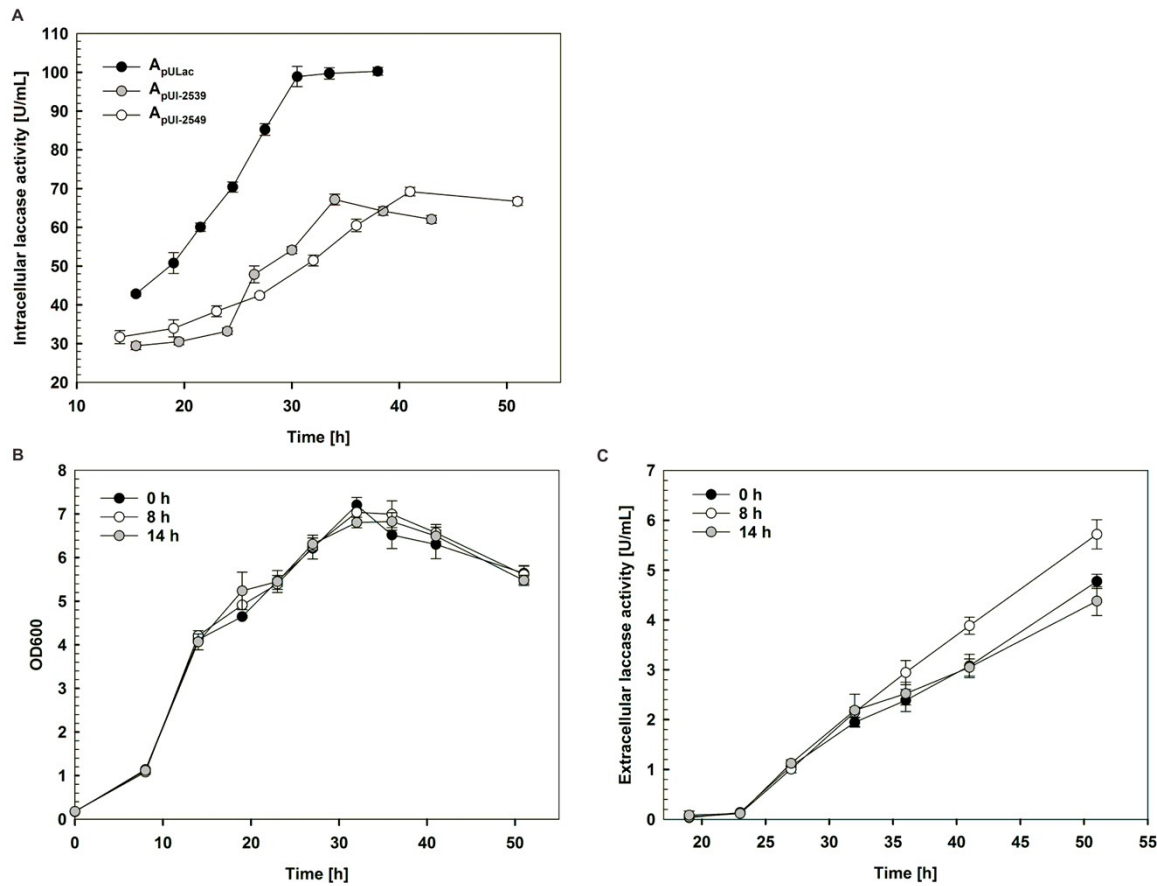


Figure S3 Periplasmic and cell-bound laccase activities for the recombinant A514 strains in TVSS strategy. (A) The real-time periplasmic laccase activities for the recombinant A514 strains with laccase integrated with different N-terminal Tat signal peptides. A_{pGlac} , which doesn't carry N-terminal signal peptides, was used as the control. (B) Whole-cell laccase activity of the recombinant A514 strains, where laccase was integrated with different β domains. N: A_{pU2816} , which doesn't carry any C-terminal regions, was used as the blank control.

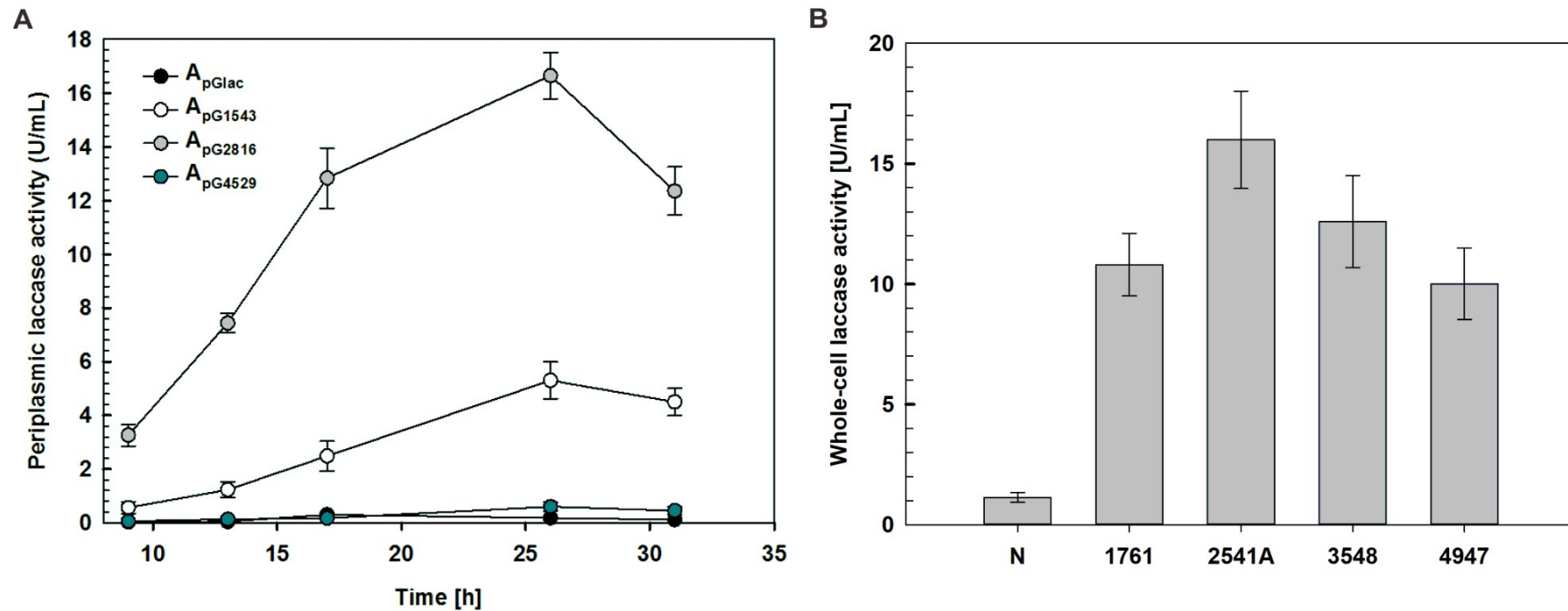


Figure S4 Definition of the optimal 2541 linker. (A) Sequential deletions of the putative linker domain. (B) The linker domain possesses a conserved α -helical region. Sequence was analyzed using Protein Calculator v 3.4. (C) Secretion efficiency of different 2541 linker regions. Analysis was performed using anti-myc ELISA. Without laccase: the passenger domain contains c-myc epitope. With laccase: the passenger domain contains c-myc epitope and laccase. (D) The cell growth (dotted line) and whole-cell laccase activities (bar) of $A_{pUV-2541A}$, $A_{pUV-2541B}$, $A_{pUV-2541C}$, and $A_{pUV-2541D}$.

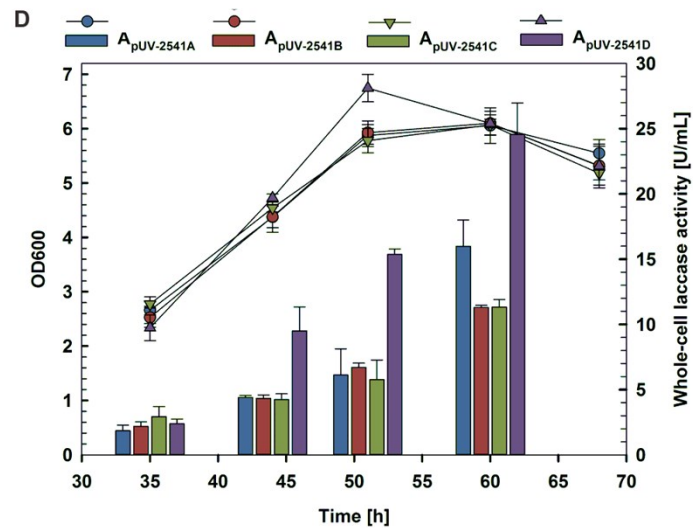
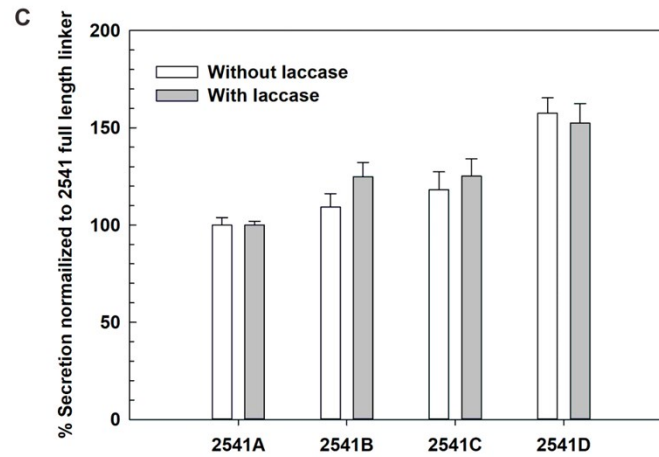
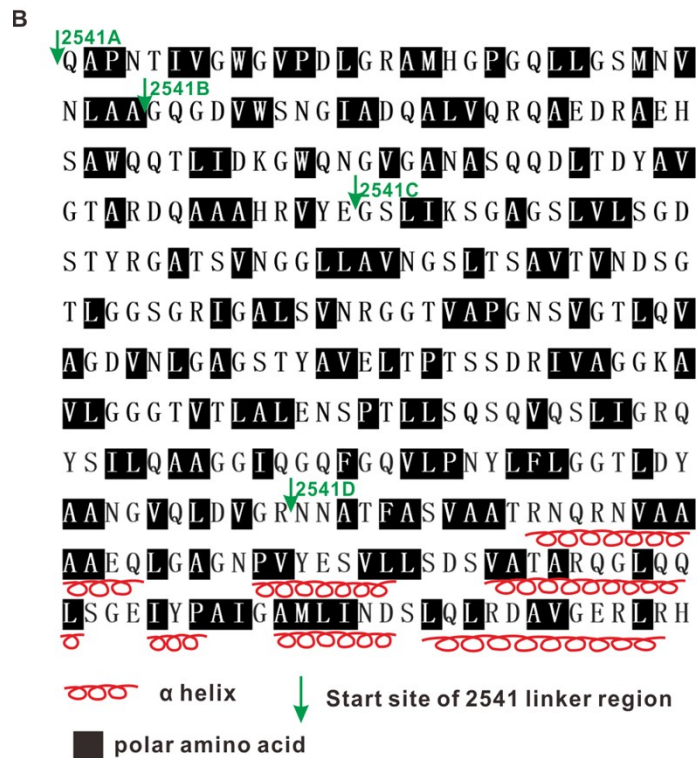
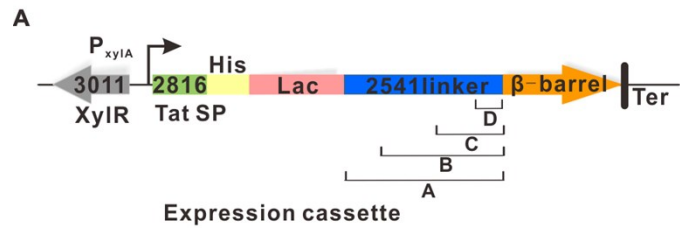


Figure S5 The proposed lignin oxidation by bacterial laccase ¹⁻⁴.

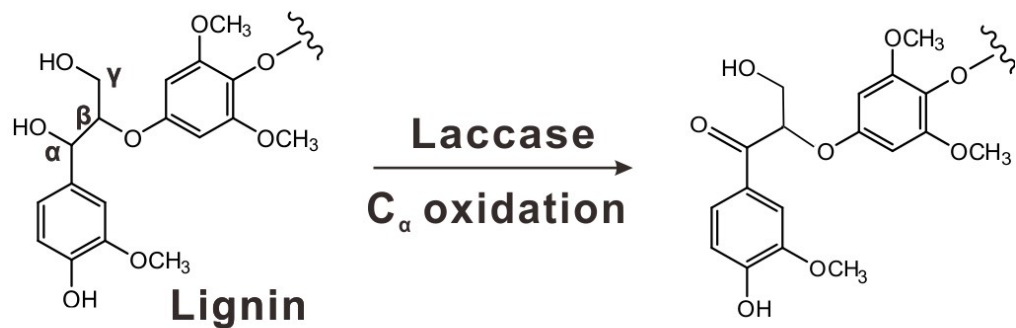


Figure S6 GPC chromatograms for untreated lignin (control), laccase alone, A_{pU} , $A_{pUI-2549}$ and $A_{pUV-2541D}$ treated lignin.

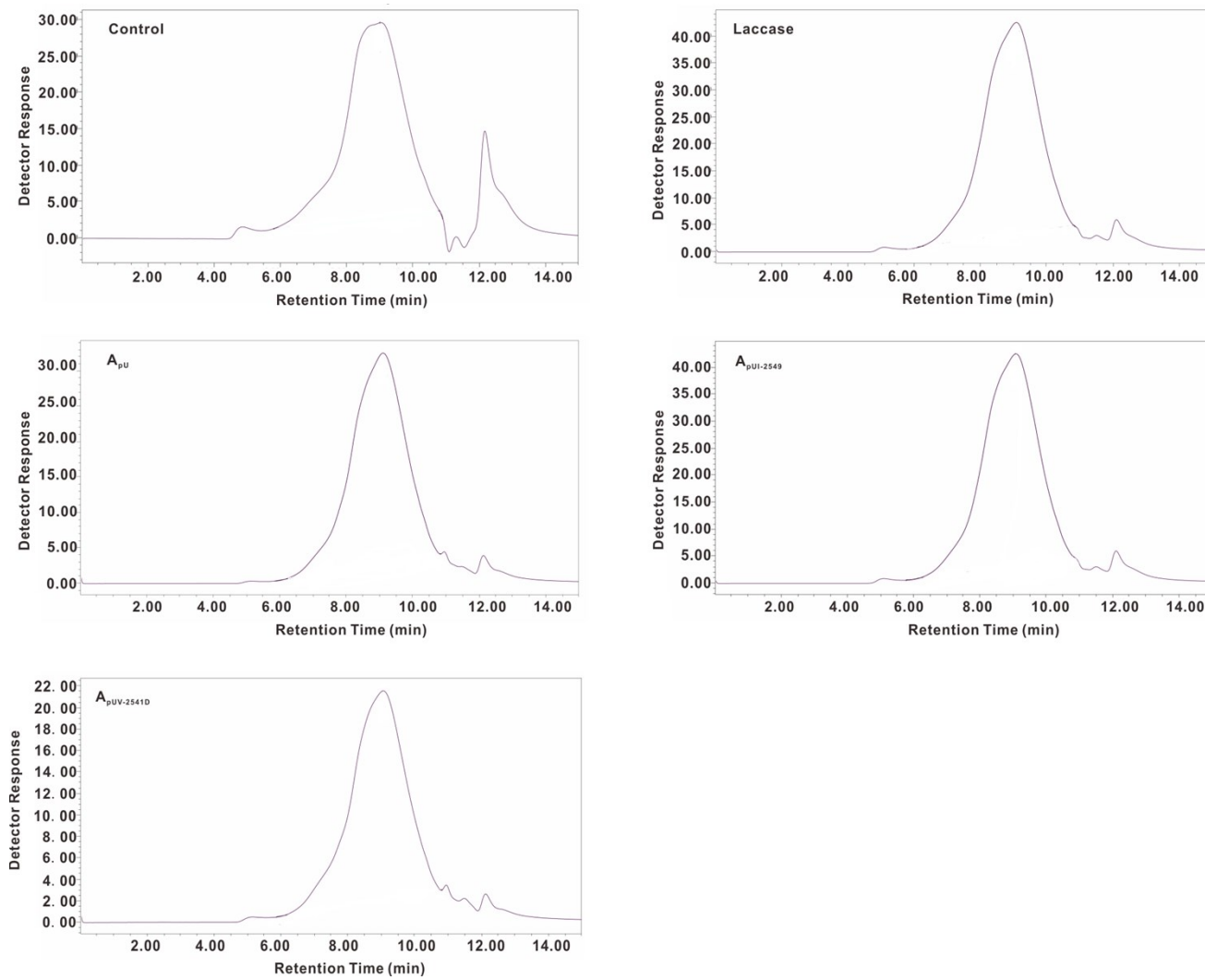
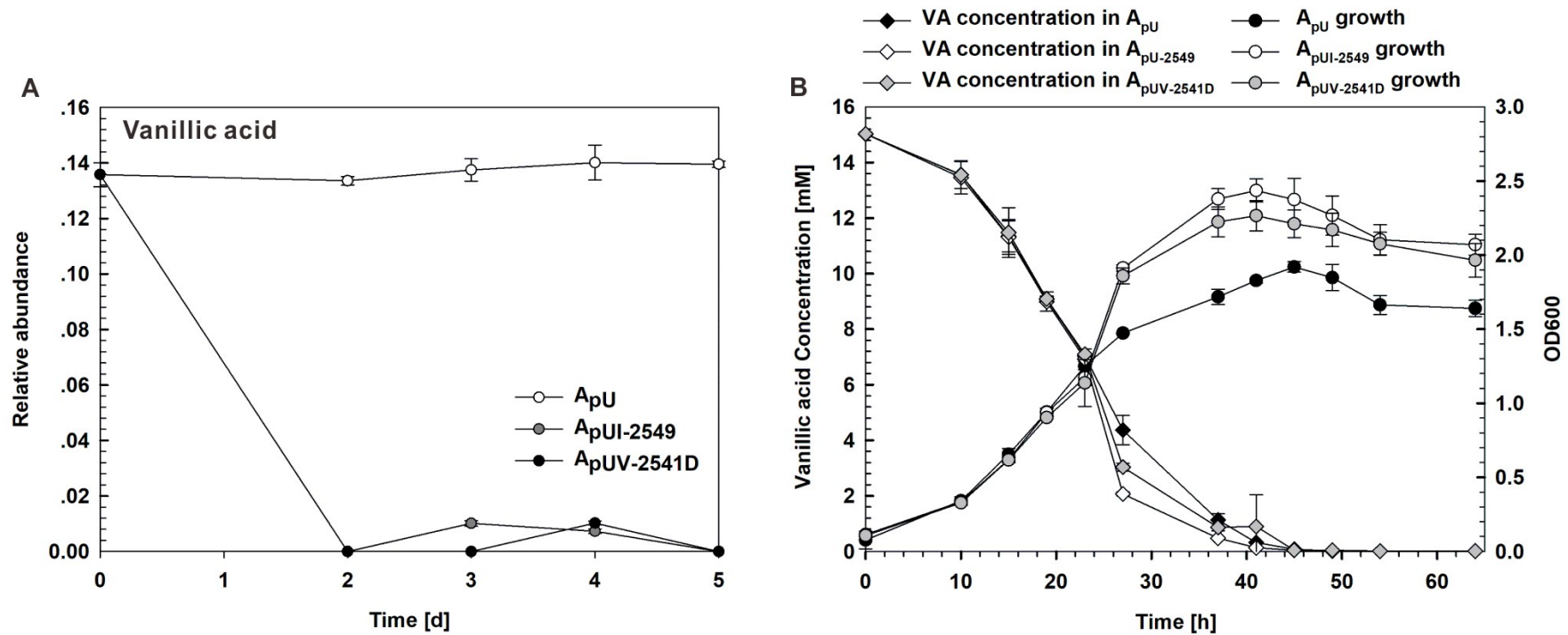


Figure S7 Vanillic acid was consumed by A_{pU} , $A_{pUI-2549}$, and $A_{pUV-2541D}$. (A) The relative abundance patterns of vanillic acid during the five cultivation days as detected by GC-MS/MS analysis. A_{pU} , $A_{pUI-2549}$, and $A_{pUV-2541D}$ were grown in lignin-M9 rich medium at 28 °C, 150 rpm. (B) Growth curves and vanillic acid degradation curves. Strains were cultured in 15 mM vanillic acid-M9 mineral medium at 28 °C and 150 rpm. VA: vanillic acid.



References:

1. R. Hilgers, J. P. Vincken, H. Gruppen and M. A. Kabel, *ACS Sustain Chem Eng*, 2018, **6**, 2037-2046.
2. G. M. Rashid, C. R. Taylor, Y. Liu, X. Zhang, D. Rea, V. Fülöp and T. D. Bugg, *ACS Chem Biol*, 2015, **10**, 2286-2294.
3. S. Majumdar, T. Lukk, J. O. Solbiati, S. Bauer, S. K. Nair, J. E. Cronan and J. A. Gerlt, *Biochemistry*, 2014, **53**, 4047-4058.
4. S. Xie, Q. Sun, Y. Pu, F. Lin and J. S. Yuan, *ACS Sustain Chem Eng*, 2016, **5**, 2215-2223.